2023

A DnaK Chaperone System Connects Type IV Pilus Activity to Polysaccharide Secretion in the Cyanobacterium Nostoc punctiforme

Heather J. McDonald
University of the Pacific

A DnaK Chaperone System Connects Type IV Pilus Activity to Polysaccharide Secretion in the Cyanobacterium *Nostoc punctiforme*

By

Heather J. McDonald

A Thesis Submitted

In Partial Fulfillment of the

Requirements for the Degree of

MASTER OF SCIENCE

College of the Pacific
Biological Sciences

University of the Pacific
Stockton, California

2024

A DnaK Chaperone System Connects Type IV Pilus Activity to Polysaccharide Secretion in the Cyanobacterium *Nostoc punctiforme*

By

Heather J. McDonald

APPROVED BY:

Thesis Advisor: Douglas Risser, Ph.D.

Committee Member: Douglas Weiser, Ph.D.

Committee Member: Craig Vierra, Ph.D.

Department Chair: Dr. Eric Thomas

A DnaK Chaperone System Connects Type IV Pilus Activity to Polysaccharide Secretion in the Cyanobacterium *Nostoc punctiforme*

By

Heather J. McDonald

Acknowledgments

First and foremost, I'd like to acknowledge and thank Dr. Doug Risser for his excellent instruction and support these last four years. The Risser lab holds students to high standards of research quality and academic integrity. I am grateful for the opportunity to learn in such a lab and work with other incredible undergraduate and graduate level researchers. My short time in the Risser lab greatly advanced my understanding of genetics and bacteriology in such a way to already significantly support my current career. Furthermore, Dr. Risser truly embodies a spirit of kindness and empathy as a professor and a PI. Thank you Dr. Risser for your example of scientific excellence and ethical leadership.

I would like to acknowledge Esthefani Zuniga for her generous support and instruction during first year of research. Esthefani went out of her way to help me through my first few months of protocols and was always patient and kind.

I would like to acknowledge the biology faculty at The University of the Pacific for their instruction and assistance during my courses and with all the random questions and advice I threw their direction. I would like to especially acknowledge my committee members Dr. Craig Vierra and Dr. Doug Wiser for their time and input. Lastly, I'd like to acknowledge Dr. Eric Thomas for his assistance during my application to the program and continued support through the Covid-19 pandemic. Thank you to all the faculty that believed in me and encouraged me through my research.

I would like to acknowledge the NSF for funding the research in this thesis.

Finally, I would like to acknowledge the friends and family that have supported me from the start. Thank you to my husband Matt for listening to hundreds of hours of presentations and

lectures with me. Thank you for supporting me emotionally and finically as we entered the pandemic together while I was in school and teaching online. This thesis is complete in no small part to your commitment and assistance.

A DnaK Chaperone System Connects Type IV Pilus Activity to Polysaccharide Secretion in the Cyanobacterium *Nostoc punctiforme*

Abstract

By Heather J. McDonald

University of the Pacific
2024

Type IV pili (T4P) systems are widely utilized among bacteria to power and direct surface motility. The production and secretion of a viscous polysaccharide to provide friction and resistance to the extended pilus structure is seen in several species of cyanobacteria including *Nostoc punctiforme*. The complex coregulation of polysaccharide secretion and T4P motor activity is not fully understood, although studies indicate a consistent relationship between functional motility and intact pathways of polysaccharide secretion and pilus extension in cyanobacteria. Using a combination of protein-protein interaction analysis, cytological studies, and comparative genomics this study proposes a theoretical mechanism for T4P motor influenced regulation of hormogonium polysaccharide secretion by a heat-shock protein (HSP) DnaK-type chaperone system in *N. punctiforme*. The results of this study indicate a tripartite HSP system consisting of DnaK1, DnaJ3, and coregulator GrpE is influenced by the activation of certain motor proteins in the T4P complex and are required for the production and secretion of hormogonium polysaccharide. Conservation of this system in *Synechocystis sp.* also implies a potential system that is conserved among all motile cyanobacteria for regulation of T4P.

Table of Contents

List of Tables

Table

List of Figures

Figure

INTRODUCTION

Significance of Cyanobacteria

Cyanobacteria are an oxygenic and photosynthetic group of ancient bacteria found in nearly every terrestrial and aqueous environment on earth. Credited as the source of the Great Oxygenation Event (GOE) in the Paleoproterozoic era, cyanobacteria rapidly raised the concentration of atmospheric oxygen (O_2) significantly altering existing abiotic conditions. When the constraints of toxic anaerobic conditions declined, multicellular organisms began to appear and evolve into more complex life-forms (Holland, 2002). As part of the oldest fossils on record appearing as early as 3 to 2.5 billion of years ago, oxygenic photosynthetic cyanobacteria served as the foundational producer in every ecosystem and remain ubiquitous today (Nisbet at al. 2007). Cyanobacteria are also integral to the global nitrogen and global carbon cycles. The enzyme nitrogenase found in cyanobacteria converts inert atmospheric nitrogen (N_2) into bioavailable nitrogen (NH_3) to be further utilized by plants. After the GOE, selective pressures of an unstable and more oxygen rich atmosphere most likely prompted the development of several morphological unique cell-types within several "classes" of cyanobacteria (Meeks & Elhai, 2002)

Within the class IV cyanobacteria Nostocales, *Nostoc punctiforme* is a multicellular filamentous cyanobacteria characterized by uni-polar mobility and four unique cell types; vegetative, heterocysts, akinetes, and hormogonia. Vegetative cells are organized into long non-motile filaments that contain membrane bound thylakoids. (Meeks & Elhai, 2002) The existence of a membrane bound organelle within cyanobacteria is often used to support the theory of endosymbiosis as the origin of photosynthesis in plant cells. (McFadden, 2014) Heterocysts are

unique nitrogen-fixing cells that function in both low and high light conditions. Heterocysts are vital to the production of soil nitrogen and allow the cyanobacteria to continue photosynthesis and nitrogen-fixation without hindering either process (Meeks et al., 2002; Adams & Carr, 1981). The repletion of soil nitrogen is required for plant growth as plants are incapable of utilizing atmospheric nitrogen and must rely on aquatic or soil bioavailability. *N. punctiforme* colonizes plants providing local nitrogenase activity thereby promoting plant growth in an otherwise nitrogen deficient environment. This symbiosis is integral to the growth and evolution of plants in every ecosystem. (Risser & Meeks, 2014 and Pratte & Thiel, 2021) Akinetes are spore-like cells that can resist desiccation and significant temperature fluctuations (Meeks et al., 2002). Akinetes may also undergo a series of biochemical changes in response to external conditions and may produce toxic aquatic blooms. Cyanobacteria are often colloquially referred to as "blue-green algae" and frequently present an environmental hazard in aquatic environments. Toxic blooms occur more frequently in polluted aquatic systems and with rising global temperatures may negatively affect local livestock and agriculture (Rastogi et al., 2015)

Gene Regulatory Network and Hormogonia

Hormogonia are motile filaments that develop in response to a number of environmental stimuli. These filaments are crucial to the establishment of plant-cyanobacterial symbioses that contribute to the global carbon and nitrogen cycles. The development of hormogonia in *N.punctiforme* is controlled by a gene regulatory network (GRN) involving a hierarchical sigma factor cascade modulated by the hybrid histidine kinase HrmK (Gonzales et al., 2019 and Zuniga et al., 2020). The GRN regulates the production of several hormogonium specific proteins key to developing fully motile and morphologically distinct cells. In addition to achieving a smaller and narrower cell shape, the development of hormogonia is also characterized by the secretion of a

viscous hormogonium polysaccharide (HPS) and by the development of bi-polar Type IV pilus structures (Castenholz et al., 1982 and Rippka et al., 2001) The histidine kinase known as HrmK is the most known upstream regulator of the induction of hormogonia (Zuniga et al., 2021). The phosphorylation of this regulatory protein stimulates, through an unknown system, a trio of sigma factors: *sigJ, sigC,* and *sigF*. These sigma factors in turn drive certain cellular processes throughout hormogonium induction. (Gonzalez et al., 2019). The most upstream of the sigma factors is *sigJ* and it serves to positively regulate *sigF* and *sigC* experiencing some reciprocal inhibition by the expression of *sigC.* T4P synthesis, signal transduction, cell division, and cytoskeletal formation all depended on the expression of these sigma factors. Knock outs of *sigC* and *sigJ* abolished cellular division and induction into hormogonium. The *sigF* knockout successfully induced phenotypical wild type (WT) hormogonia, however, mutant *sigF* strains were unable to produce detectable levels of PilA. This model implies *sigF* may act further downstream to its counterparts (Gonzales et al. 2019).

Type 4 Pilus

Movement of hormogonia is unidirectional and photosensitive. *N. punctiforme* extends the T4P towards the direction of motility, establishing a leading and lagging pole. The T4P system is arrayed into static bipolar rings that contain a series of key functional proteins that aid in the secretion and retraction of the small fibril protein PilA. PilA is synthesized after hormogonium induction and then secreted to form the pilus-like structure that extends towards the direction of movement (Schuergers & Mullineaux 2017; Yegorov at al. 2021; Harwood et al. 2021; Schuergers et al. 2017). PilB and PilT are motor proteins that interact with PilC to drive the assembly of the monomeric pilus and are anchored to the inner cytoplasmic membrane extending into the cytoplasm. RNA-binding protein Hfq is also essential to hormogonium

motility and the extension of the T4P. Hfq interacts with motor protein PilB and maintains a static position at each cell pole regardless of light exposure (Schuergers et al., 2014 and Harwood et al., 2021).

Figure 1

Gene Regulatory Network

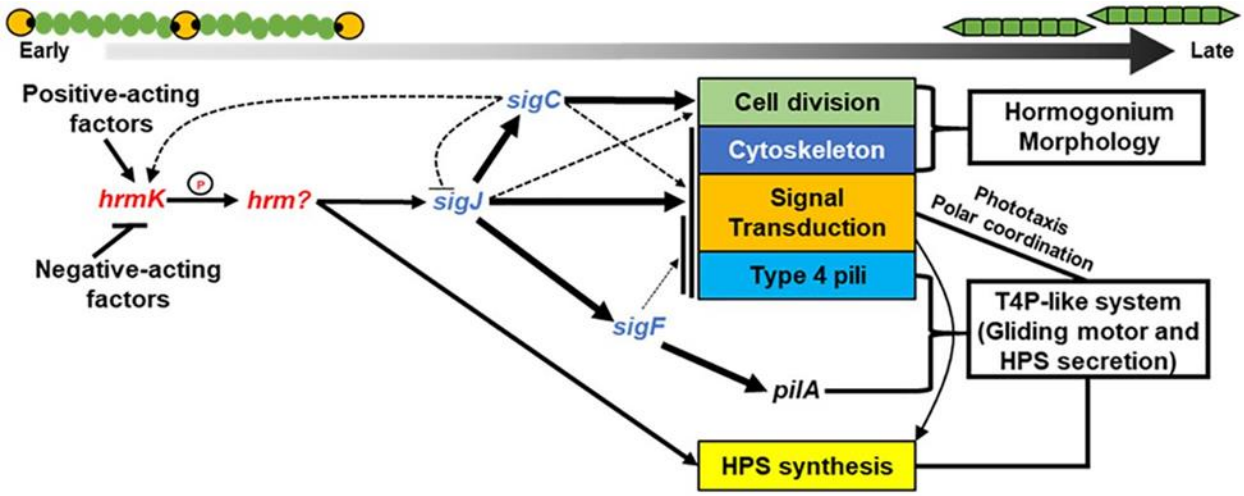

Note. Previously hypothesized working model of the gene regulatory network for hormogonium development in *N. punctiforme* (Gonzales et al., 2019).

Hmp and Ptx Systems

N. punctiforme displays positive phototaxis with a leading and lagging pole controlled by a Ptx system containing methyl accepting chemotaxis proteins (MCPs) with cyanobacteriochrome sensory domains that perceive light (Risser et al., 2014). Disruption of the Ptx system within *N. punctiforme* abolishes any phototactic response resulting in non-specific uniform filament movement. The wild-type motility of hormogonia in *N. punctiforme* is unidirectional, however spontaneous switching of the leading and lagging poles of motile filaments has been observed in non-specific white light conditions (Riley et al., 2018; Harwood & Zuniga et al., 2021; Cho et al., 2017; Jakob et al., 2020). A recent study suggests that hormogonium filaments change direction from their previous trajectory when white light is removed and then restored. This directional switch is evidence for further influence over the T4P by the Ptx system (Harwood & Zuniga et al., 2021)

The chemotaxis-like Hmp system is essential for hormogonium motility in *N. punctiforme*. The deletion of gene *hmpF* within the *hmp* locus completely abolished hormogonium motility and is characterized by the lack of secreted extracellular HPS and PilA. (Harwood & Zuniga et al., 2021) While the exact function of HmpF is unknown, recent studies have shed light on the unique dynamic localization properties of the protein in hormogonia. HmpF has been shown to accumulate to the leading pole in hormogonia in normal light conditions. However, when the light source is removed HmpF will dissociate from the lagging pole and diffuse into the cytoplasm losing polar specificity. When the light source is restored HmpF will once again aggregate to the lagging-pole - essentially switching poles. This light response of HmpF suggests a possible direct relationship between the Ptx system and the chemotaxis-like Hmp system. Furthermore, HmpF directly interacts with T4P proteins Hfq,

PilT1 and PilT2. The Hmp system is believed to coordinate the polarity of HmpF to establish motility while the Ptx system modulates reversal in response to changes in light intensity (Harwood & Zuniga et al., 2021 and Cho et al., 2017)

Hormogonium Polysaccharide

Forward movement of *N. punctiforme* is also facilitated by the synthesis and secretion of a fucose-specific hormogonium polysaccharide (Khayatan et al., 2015). The viscous polysaccharide provides resistance during retraction of the T4P-like structure pulling the hormogonium filaments forward. Synthesis of hormogonium polysaccharide is regulated by several *hps* loci with several shown to be crucial to hormogonium motility and accumulation of extracellular hormogonium polysaccharide (Risser & Meeks, 2013; Zuniga et al., 2020; Khayatan et al., 2015). Additionally, the *hps* locus (*hps A-K*) encodes for glycosyltransferases, psudo-pillins/minor pillins and proposed membrane proteins which are upregulated in hormogonium development with notable exceptions *hpsE-G* which are upregulated in hormogonia independent of sigma factor expression (Risser & Meeks, 2013). The involvement of pseudo-pilin and minor pilin proteins is typically associated with type II and type IV secretion systems. Previous research also shows that functional extension and retraction of the T4P system in *N. punctiforme* is essential for extracellular hormogonium polysaccharide accumulations. These findings together suggest that hormogonium polysaccharide may be exported across the cell membrane by a T2P/T4P-like system. Further analysis of extracellular polysaccharide secretion in gram-negative cyanobacteria reveals a complex multi-step synthesis and export processes. (Risser and Meeks, 2013; Khayatan et al., 2015)

The other competing hypothesis of how hormogonium polysaccharide is secreted proposes a mechanism of secretion that includes the transport of oligosaccharide units across the

cell membrane by a Wzx-type flippase. The repeating units are then further polymerized by Wzy polymerase in the periplasm before exiting through outer membrane channels formed by Wza. A recent study has identified several additional loci involved in hormogonium polysaccharide secretion containing most of the components required for the assembly of a Wzx/Wzy-type export system in *N. punctiforme* (Zuniga et al., 2020).

Heat Shock Proteins DnaK and DnaJ

An ongoing transposon mutagenesis study to identify genes essential for hormogonium motility and development in *N. punctiforme* (Khayatan et al., 2017) identified a non-motile strain (TNM719) with transposon insertions in the gene Npun_F0122 (*dnaK1*). This *dnaK1* encodes for a type of heat shock protein of the class HSP70 also known as DnaK. HSP70 is a highly conserved molecular chaperone found in nearly every prokaryotic and eukaryotic organism. The prokaryotic homologue of HSP70, DnaK, primarily functions as an ATPase that assists in the folding of denatured proteins through protein-protein interactions in tandem with co-chaperone DnaJ (HSP40) and GrpE. GrpE is a nucleotide exchange factor that promotes the dissociation of adenosine diphosphate (ADP) from DnaK. GrpE is often involved and upregulated in direct response to elevated temperatures and is historically found within bacterial cell membranes. DnaJ proteins are highly diverse, and cyanobacteria often contain several homologs as well. DnaJ functions to define the protein specificity of DnaK and interacts with both the protein of interest and DnaK directly. (Mayer & Giersch., 2019; Sugimoto et al., 2021; Ruppresch et al., 2007). The functional DnaJ domain known as the J-box directly binds to DnaK while the C-terminal domain of DnaJ is highly specific and interacts only with the protein of interest. The HSP70 system is widely studied within many species of bacteria under numerous stress conditions not limited to drought tolerance, temperature fluctuations, and nutrient

deprivation (Mayer & Giersch., 2019; Sugimoto et al., 2021; Ruppreschtet al., 2007, Xu et al., 2020). The first step in refolding of denatured proteins is the recognition and sequential binding of DnaJ to sections of an unfolded protein. DnaK then binds to DnaJ by ATP-hydrolysis forming a triple protein complex that interacts with the unfolded protein. DnaK is released through a conformational change initiated by nucleotide exchange factor protein GrpE releasing ADP from DnaK and allowing ATP to rebind. This cycle of binding repeats until the protein is fully reformed and DnaJ can no longer interact with the specific unfolded protein section (Sugimoto et al., 2021 and Xu et al., 2020). With identification of the potentially crucial gene *dnaK1* as a heat shock protein, further identification of the obligatory cognate partners DnaJ and GrpE, as is generally understood in similar bacterial models, is imperative to understanding the role and function of DnaK within the hormogonia gene regulatory network (Mayer & Giersch., 2019; Sugimoto et al., 2021; Ruppreschtet al., 2007).

Previous studies of the heat-shock proteins in cyanobacteria suggest that DnaK may also be highly localized within the cell. Xu et al. found that a protein analogous to HSP70, identified as NfDnaK2, in *Nostoc flagelliforme* was upregulated during desiccation stress (2020). A yeast-two-hybrid analysis of eleven potential DnaJ proteins identified NfDnaJ9 as the only co-chaperone of NfDnaK2. The subcellular location of NfDnaK2 was further investigated through western blot analysis of the plasma membrane, thylakoid membranes, and soluble proteins. Of the three potential locations, NfDnaK2 was only found in the thylakoid membranes and upon transcriptomic analysis accounted for over 94% of all DnaK reads in the dehydrated strains. Additionally, heterologous expression of NfDnaK2 in *N. flagelliforme* enhanced drought tolerance of the species. Given the location and apparent essential function of NfDnaK2 – NfDnaJ9 a GST-tag pull-down assay of co-chaperone NfDnaJ9 was conducted and the protein

protease NfFstH2 was identified as a potential target substrate. NfFstH2 is a known protease involved in the repair cycle of Photosystem II by way of damaged D1 protein degradation. Potential other functions protein targets for NfFstH2 were not identified in the study. However, several other DnaK homologs were also identified and found to be highly localized within *N. flagelliforme* and were either constitutively expressed or upregulated at different points of the cell cycle unrelated to desiccation (Xu et al., 2020). Evidence of this type of highly specified localization further suggests a diverse range of functions for the HSP70 systems within cyanobacteria (Fig. 2).

Figure 2

DnaJ/DnaK/GrpE Reaction Cycle

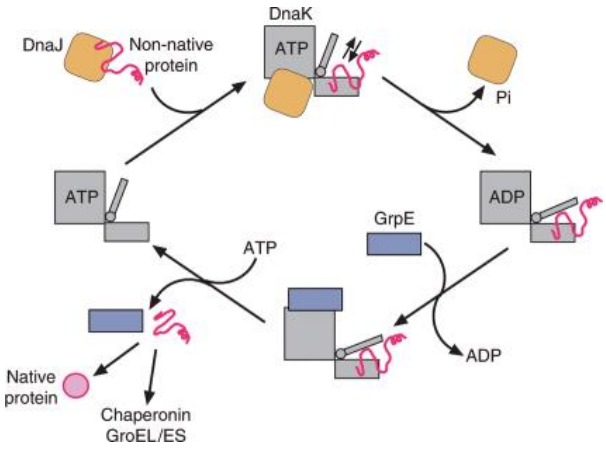

Note. Depiction of typical Dnak/DnaJ/GrpE reaction cycle in *Escherichia coli* (*E. coli*). DnaJ captures the substrate protein and transfers it to DnaK in the ATP-bound state. DnaJ and substrate synergistically trigger ATP hydrolysis by DnaK, thereby generating a stable complex between the substrate and DnaK in the ADP-bound state. Catalysis of ADP-ATP exchange by GrpE stimulates substrate release and regenerates DnaK-ATP for another round (Rahmi et al., 2020).

Proteostasis

Other recent studies also suggest that the HSP70 system is also heavily involved in regulatory cell functions and proteostasis in cyanobacteria. The biogenesis of thylakoid membranes and the maintenance of the thylakoid membrane-localized electron transport proteins within cyanobacteria *Synechocystis sp*. was dependent on the background expression of an HSP70 protein coined DnaK3 (Thurotte et al., 2020). Several homologs of *dnaJ* found in a cluster were unable to be deleted in *Synechococcus sp.* implying an essential function outside of obvious stress conditions. While most of the DnaJ-DnaK protein interactions are largely unknown within cyanobacteria, it is important to note the wide variety of conditions and functions these proteins serve in regulating a significant variety of cellular responses (Thurotte et al., 2020)

Additionally, the lack of heat-stress within the hormogonium induction process of *N. punctiforme* implies a regulatory or stress mitigation function of *dnaK1* independent of temperature conditions. Research by Morioka et al. further emphasizes the proteoregulatory function of the HSP70 system elucidating the role of HSP70 in curli production by *E. coli*. J-domain proteins (JDP) were found to be essential in the production of curli proteins in non-stress conditions (2014). With either the full or partial deletion of certain JDP, curli production was severely inhibited or eliminated altogether. This study also further explored the regulatory relationship between DnaK and DnaJ, emphasizing a lack of binding site specificity for DnaK. This lack of specificity is believed to contribute to the speed of reaction of the HSP70 system and the multiple and varied protein interactions observed with a single DnaK. Genomes of both *E. coli* and cyanobacteria contain less DnaK homologues than DnaJ in line with the theory a wide and variable function for JDP (Morioka et al., 2014).

MATERIALS AND METHODS

Plate Motility Assay

WT and mutant strains were streaked onto AA/4 plates containing 10 mM sucralose. Individual colonies were then picked and spotted onto AA/4 plates containing 0.5% Noble agar. Plates were incubated at room temperature under continuous light for 48 h, and then colonies were imaged using a Leica MZ APO dissecting microscope equipped with a Leica DFC290 camera controlled by Micro-Manager imaging software. Each assay was repeated for a total of three replicates per sample (Edelstein et al. 2014).

Bacterial-Two-Hybrid

The coding regions of *dnaJ* and *dnaK* genes were amplified using PCR and cloned into the pUT18/pUT18c and pKT25/PKNT25 vector. The final plasmids, which expressed proteins with DnaJs and DnaK1 fused to either the N or C terminus of fragments T18 and T25 of adenylate cyclase were co-transformed into BTH101 *Escherichia coli* cells. The cells were streaked onto plates containing lysogeny broth (LB) + 100ug/mL ampicillin and 50ug/mL kanamycin and isopropyl β-D-1-thiogalactopyranoside incubated at 30°C for 24 hours. Cells were then collected from multiple colonies and used to inoculate a 2mL LB solution containing that same concentrations of ampicillin and kanamycin with and incubated with agitation for another 24 hours. 2 µl of cell cultures were spotted on MacConkey agar and incubated for 24-48 hours before reading for results (Karimova et al., 1998; Battesti & Bouveret, 2012; Zhang & Bremmer, 1995; Riley et al., 2018).

Strains and Culture Conditions

N. punctiforme ATCC 29133 and its derivatives were cultured in Allan and Arnon medium diluted fourfold (AA/4), without supplementation of fixed nitrogen, as previously described (Campbell et al. 2007), with the exception that 4 and 10 mM sucralose was added to liquid and solid medium, respectively, to inhibit hormogonium formation (Splitt & Risser 2015). For small scale hormogonium induction for phenotypic analysis, the equivalent of 30 μg ml-1 chlorophyll a (Chl a) of cell material from cultures at a Chl a concentration of 10-20 μg ml^{-1} was harvested at 2,000 g for 3 min, washed two times with AA/4 and resuspended in 2 ml of fresh AA/4 without sucralose. For large scale hormogonium induction for RT-qPCR analysis, this process was repeated, but starting with the equivalent of 300 μg ml-1 Chl a of cell material and resuspension in 50 ml of fresh AA/4. For selective growth, the medium was supplemented with 50 μg ml^{-1} neomycin. *Escherichia coli* cultures were grown in lysogeny broth (LB) for liquid cultures or LB supplemented with 1.5% (w/v) agar for plates. Selective growth medium was supplemented with 50 μg ml-1 kanamycin, 50 μg ml^{-1} ampicillin, and 15 μg ml^{-1} chloramphenicol.

Plasmid and Strain Constructions

All constructs were sequenced to insure fidelity.

To construct plasmids for in-frame deletion of target genes, approximately 900 bp of flanking DNA on either side of the gene and several codons at the beginning and end of each gene were amplified via overlap extension PCR (Tables 1 and 2 for details) and cloned into pRL278 (Cai & Wolk 1990) as BamHI-SacI fragments using restriction sites introduced on the primers.

To construct mobilizable shuttle vectors containing *dnaK1* or *dnaJ3* and its putative promoter region, the coding-region and 200 bp upstream of the TSS (Harwood & Risser 2021) was amplified via PCR and subsequently cloned into pAM504 (Wei et al. 1994) as BamHI-SacI fragments using restriction sites introduced on the primers.

To construct plasmid pDDR503 for replacement of the chromosomal allele of *dnaK1* with a C-terminal *gfpuv*-tagged variant, approximately 900 bp of DNA downstream of the stop codon were amplified via PCR and cloned into pSCR569 (Risser at al. 2015), as an SpeI-SacI fragment using restriction sites introduced on the primers. Approximately 900 bp of DNA upstream of the stop codon were then amplified via PCR and cloned into this plasmid as a BamHI-SmaI fragment using restriction sites introduced on the primers.

To construct plasmid pDDR506 for replacement of the chromosomal allele of *dnaJ3* with a C-terminal *gfpuv*-tagged variant, approximately 900 bp of DNA downstream of the stop codon were amplified via PCR and cloned into pSCR569 (Risser et al. 2012), as an SpeI-SacI fragment using restriction sites introduced on the primers. The coding region of *dnaJ3* and approximately 900 bp of DNA upstream of the start codon were then amplified via PCR and cloned into this plasmid as a BamHI-SmaI fragment using restriction sites introduced on the primers.

To construct plasmids encoding proteins of interest fused to either the T18 or T25 fragment of Bordetella pertussis adenylate cyclase for BACTH analysis (Karimova et al,. 1998, Battesti & Bouveret 2012), the coding region of each gene was amplified via PCR and cloned into either pUT18/pUT18c or pKT25/pKNT25 using restriction sites introduced on the primers (see Table 2 for details on restriction sites used for each gene).

Generation of transposon mutants and identification of transposon insertion sites was performed as previously described (Khayatan et al. 2017) using plasmid pRL1063a (Wolk et al. 1991). Gene deletions and allelic replacements were performed as previously described (Risser & Meeks 2013) with *N. punctiforme* cultures supplemented with 4 mM sucralose to inhibit hormogonium development and enhance conjugation efficiency (Khayatan et al 2017, Splitt & Risser 2015). To construct UOP176, UOP201, and UOP 202, plasmids pDDR475, pDDR501, and pDDR503 were introduced into wild type *N. punctiforme* ATCC29133, respectively. To create UOP211, plasmid pDDR424 (Cho et al. 2017) was introduced into UOP201. To construct UOP213, plasmid pDDR506 was introduced into UOP202 and maintained as a single recombinant with selection on neomycin because counter-selection on 5% sucrose repeatedly failed to yield any double-recombinant colonies with the *dnaJ3-gfp* allele.

Fluorescence Microscopy

Fluorescence microscopy was performed with an EVOS FL fluorescence microscope (Life Technologies) equipped with a 10x or 63x objective lens. Excitation and emission were as follows: EVOS™ light cube, GFP (AMEP4651: excitation 470+/-22 nm, emission 525+/-50 nm) for UEA-fluorescein labeled HPS; EVOS™ Light Cube, DAPI (AMEP4650: excitation 357+/-44 nm, emission 447+/-60 nm) for immunofluorescence labeled PilA; EVOS™ light cube, Nrw 405 (AMEP4857: excitation 390+/-18 nm, emission 525+/-50 nm) for GFPuv; and EVOS™ Light Cube, RFP (AMEP4652: excitation 531+/-40 nm, emission 593+/-40 nm) for cellular autofluorescence. To image immobilized filaments expressing GFP fusion proteins 5µl of culture were placed on a dehydrated 1% agarose pad on a glass slide and overlaid with a cover slip. To image mobile filaments wet mounts were prepared using 10 µl of culture on a glass slide overlaid with a cover slip. For treatment with carbonyl cyanide m-chlorophenyl hydrazine

(CCCP), 1 µl of 10 mM CCCP in DMSO, or DMSO alone was added to 1 ml of culture and incubated for 15 minutes. Subsequently, 5 µl of culture were placed on a hydrated 1% agarose pad containing 10 µM CCCP, or DMSO alone and overlaid with a coverslip.
Quantification of polar and cytoplasmic fluorescence derived from GFP-fusion proteins was performed using imageJ (NIH). A line was drawn perpendicular to the long axis of the filament across the width of the cell junction or the middle of the cell for 5 contiguous cells for each of 5 filaments from 3 biological replicates and the average pixel intensity was measured for these regions.

Light Microscopy

10µl of each sample were spotted on a slide containing dehydrated 1% agarose pads. Samples were imaged at 400x using a Leica DME microscope attached to a Leica DFC290 camera controlled by Micro-Manager imaging software, and images were then analyzed using ImageJ software. 50 filaments were chosen at random and the presence/absence of heterocysts and average cell length from five contiguous vegetative cells were determined for each filament, in order to calculate the percent of total filaments with heterocysts and average vegetative cell length for each strain at 0 h and 24 h post-induction. Each induction was repeated for a total of three replicates per sample (Edelstein et al. 2014).

Western Blot

Standard SDS-PAGE and previously described immunoblot procedures were followed (Risser, Chew, Meeks 2014; Wall, Wu, Kaiser 1998) using primary anti-PilA, anti-HmpD, and anti-RbCL rabbit polyclonal antisera in a 1:10,000 dilution, and horseradish peroxidase (HRP)-conjugated goat anti-rabbit secondary antibodies (Chemicon) in a 1:20,000 dilution. Enhanced chemiluminescent (ECL) detection of immunoblots was performed by addition of Clarity™

Western ECL blotting substrate (Bio-Rad Laboratories) and imaging in a Bio-Rad Molecular Imager ChemiDoc™ XRS+. Quantitative analysis of the immunoblot was completed using ImageJ software. Each blot was repeated for a total of three replicates per sample (Cho et al., 2017)

Lectin Blot

Supernatants of hormogonium from each mutant and WT strain were collected at 24 hrs post inductions and stored at 4C. 100 µl of each supernatant sample were vacuum blotted onto a wet nitrocellulose membrane and subsequently dried at 55°C for 5 min. The membrane was blocked for 30 min at room temperature with shaking at 50 rpm in Carbo-Free™ Blocking Solution (Vector Laboratories), and then incubated for 1h at room temperature with shaking (50 rpm) in a Tris-buffered saline + 0.1% Tween20 (TBST) wash solution containing 0.5 µg/ml of biotinylated-*Ulex europaeus* agglutinin (UEA) lectin. The membrane was then washed 3 times in TBST, followed by incubation for 1 h at room temperature with gentle shaking (50 rpm) in VECTASTAIN® ABC reagent (Vector Laboratories). The membrane was again washed 3 times in TBST, followed by one wash in Tris-buffered saline (TBS). ECL detection of lectin blots was performed by addition of Clarity™ Western ECL blotting substrate (Bio-Rad Laboratories) and imaging in a Bio-Rad Molecular Imager ChemiDocTM XRS+. Quantitative analysis of lectin blots was performed using ImageJ. Each blot was repeated for a total of three replicates per sample (Cho et al., 2017).

Table 1

Strains and Plasmids Used in This Study

Strains	Relevant Characteristic(s)	source
Nostoc punctiforme strains		
ATCC 29133	wild type	ATCC
UCD153	Laboratory derivative of *N. punctiforme* ATCC 29133 with reduced motility	(Campbell et al. 2007)
UOP176	Δ*dnaK1* (Npun_F0122) *	This study
UOP202	Δ*dnaJ3* (Npun_F1160)	This study
TNM719	UCD153 with a Tn5-1063 insertion after nucleotide 754 of *dnaK1*	This study
TNM14173	UCD153 with a Tn5-1063 insertion after nucleotide 845 of *dnaK1*	This study
UOP201	*dnaK1-gfp*	This study
UOP211	*dnaK1-gfp,* ¯*hmpF*	This study
UOP213	*dnaJ3-gfp* single recombinant strain, neo^r	This study
Plasmids		
pAM504	Mobilizable shuttle vector	(Wei et al. 1994)
pRL278	Mobilizable suicide vector	(Cai et al. 1990)
pRL1063a	Suicide vector carrying Tn5-1063, a Tn5 derivative transposon	(Wolk et al. 1991)
pSCR569	Mobilizable suicide vector for C-terminal *gfpuv* translational fusions	(Risser et al. 2012)
pDDR475	Suicide vector for in-frame deletion of *dnaK1* [1-4] †	This study
pDDR501	Suicide vector for in-frame deletion of *dnaJ3* [5-8]	This study
pDDR424	Suicide vector for in-frame deletion of *hmpF*	(Cho et al. 2017)
pDDR503	Suicide vector for allelic substitution of *dnaK1* with *dnaK1-gfpuv* [4,9-11]	This study
pDDR506	Suicide vector for allelic substitution of *dnaJ3* with *dnaJ3-gfpuv* [5,8,12,13]	This study
pDDR507	Shuttle vector containing *dnaK1* and the 540 bp 5' to the start codon [14-15]	This study
pDDR508	Shuttle vector containing *dnaJ3* and the 239 bp 5' to the start codon [16-17]	This study
pEZ105	pUT18-*hfq*	(Harwood et al. 2021)
pEZ106	pUT18c-*hfq*	(Harwood et al. 2021)
pEZ109	pUT18-*pilB*	(Harwood et al. 2021)
pEZ110	pUT18c-*pilB*	(Harwood et al. 2021)
pTVH105	pUT18-*hmpF*	(Harwood et al. 2021)
pTVH106	pUT18c-*hmpF*	(Harwood et al. 2021)
pDDR480	pUT18-*hfq* (ssr3341, *Synechocystis sp.* strain PCC6803)	(Harwood et al. 2021)
pDDR481	pUT18c-*hfq* (ssr3341, *Synechocystis sp.* strain PCC6803)	(Harwood et al. 2021)
pDDR486	pUT18-*pilT1*	(Harwood et al. 2021)
pDDR487	pUT18c-*pilT1*	(Harwood et al. 2021)
pDDR490	pUT18-*pilT2*	(Harwood et al. 2021)
pDDR491	pUT18c-*pilT2*	(Harwood et al. 2021)
pHJM100	pKT25-*dnaK1* [18-19]	This study
pHJM101	pKNT25-*dnaK1* [18-19]	This study
pHJM102	pUT18-*grpE* (Npun_F0121) [20-21]	This study
pHJM103	pUT18c-*grpE* [20-21]	This study
pHJM104	pUT18-*dnaJ1* (Npun_R0986) [22-23]	This study
pHJM105	pUT18c-*dnaJ1* [22-23]	This study
pHJM106	pUT18-*dnaJ2* (Npun_F2810) [24-25]	This study
pHJM107	pUT18c-*dnaJ2* [24-25]	This study

(Table 1 Continued)

pHJM108	pUT18-*dnaJ3* (Npun_F1160) [26-27]	This study
pHJM109	pUT18c-*dnaJ3* [26-27]	This study
pHJM110	pUT18-*dnaJ4* (Npun_R3872) [28-29]	This study
pHJM111	pUT18c-*dnaJ4* [28-29]	This study
pHJM112	pUT18-*dnaJ6* (Npun_R5997) [30-31]	This study
pHJM113	pUT18c-*dnaJ6* [30-31]	This study
pHJM114	pUT18-*dnaJ7* (Npun_R5579) [32-33]	This study
pHJM115	pUT18c-*dnaJ7* [32-33]	This study
pHJM116	pUT18-*dnaJ8* (Npun_R1936) [34-35]	This study
pHJM117	pUT18c-*dnaJ8* [34-35]	This study
pHJM118	pUT18-*dnaJ9* (Npun_R6085) [36-37]	This study
pHJM119	pUT18c-*dnaJ9* [36-37]	This study
pHJM120	pUT18-*dnaJ10* (Npun_F0150) [38-39]	This study
pHJM121	pUT18c-*dnaJ10* [38-39]	This study
pHJM122	pUT18-*dnaJ11* (Npun_F0123) [40-41]	This study
pHJM123	pUT18c-*dnaJ11* [40-41]	This study
pHJM124	pUT18-*dnaJ12* (Npun_F0151) [42-43]	This study
pHJM125	pUT18c-*dnaJ12* [42-43]	This study
pHJM126	pUT18-*dnaJ13* (Npun_F2991) [44-45]	This study
pHJM127	pUT18c-*dnaJ13* [44-45]	This study
pHJM128	pUT18-*dnaJ14* (Npun_F5908) [46-47]	This study
pHJM129	pUT18c-*dnaJ14* [46-47]	This study
pDDR509	pKT25-*dnaK1syn* (sll0058, *Synechocystis sp.* strain PCC6803) [48-49]	This study
pDDR510	pKNT25-*dnaK1syn* (sll0058, *Synechocystis sp.* strain PCC6803) [48-49]	This study
pDDR511	pUT18-*pilBsyn* (slr0063, *Synechocystis sp.* strain PCC6803) [50-51]	This study
pDDR512	pUT18c-*pilBsyn* (slr0063, *Synechocystis sp.* strain PCC6803) [50-51]	This study
pDDR513	pUT18-*dnaJ3syn* (sll1384, *Synechocystis sp.* strain PCC6803) [52-53]	This study
pDDR514	pUT18c-*dnaJ3syn* (sll1384, *Synechocystis sp.* strain PCC6803) [52-53]	This study

* locus tag and genes derived from *Synechocystis* sp. strain PCC6803 rather than *N. punctiforme* denoted in parentheses

† numbers in brackets correspond to primers used to construct plasmid. Detailed information on primers can be found in Table 2

Table 2

Primers Used in This Study

Primer Name	Sequence	Primer Number	qPCR target
NpF0122-5'-F	ATATAGGATCCATGAAGAGTGACTCTCCAGC	1	
NpF0122-5'-R	cctaatctatTTTTCCCATAGTCGCCAG	2	
NpF0122-3'-F	ctatgggaaaaATAGATTAGGGATTGGGTAATG	3	
NpF0122-3'-R	ATATAGAGCTCAGCGCGGGTTTCTGGTTC	4	
NpF1160-5'-F	atataggatccCAATGCCCAATAACAAATGAC	5	
NpF1160-5'-R	cttcccGAAAGACATATAGACTTTTTGCAC	6	
NpF1160-3'-F	gtctatatgtctttcGGGAAGAAAAAATAATGGTGTATC	7	
NpF1160-3'-R	atatagagctcCCCCAAAAGTTGGTCATAG	8	
NpF0122-gfp-5'-F	atataggatccCAAAGCTCCCGATCGCTC	9	
NpF0122-gfp-5'-R	atatacccgggAATCTATCGCCTCATAATCAAC	10	
NpF0122-gfp-3'-F	atataactagtGGATTGGGTAATGGGTAATG	11	
NpF1160-gfp-5'-R	atatacccgggATTTTTTCTTCCCACCAAACAAAC	12	
NpF1160-gfp-3'-F	atataactagtTGGTGTATCAGCCAGCATC	13	
PNpF0122-BamHI-F	atataggatccTCAAACCTCAATCTGATGG	14	
NpF0122-SacI-R	atatagagctcCTAATCTATCGCCTCATAATC	15	
PNpF1160-BamHI-F	atataggatccGGGATAATTTTGTTGCAAGAAGC	16	
NpF1160-SacI-R	atatagagctcTTATTTTTTCTTCCCACCAAACAAAC	17	
NpF0122-TH-BamHI-F	atataggatcccATGGGAAAAGTTATTGGAATCG	18	
NpF0122-TH-KpnI-R	atataggtacccgATCTATCGCCTCATAATCAAC	19	
NpF0121-TH-BamHI-F	atataggatcccATGAAGAGTGACTCTCCAG	20	
NpF0121-TH-KpnI-R	atataggtacccgACTGTTGGCTGGACTCGAC	21	
Npun_R0986-TH-BamHI-F	atataggatcccATGGATCTTGGAGATTGCTAC	22	
Npun_R0986-TH-KpnI-R	atataggtacccgAAAAATTTGTTCTAAGCGTTGG	23	
Npun_F2810-TH-BamHI-F	atataggatcccATGGTCAATTCTAAGCACG	24	
Npun_F2810-TH-KpnI-R	atataggtacccgTATAACAGATGCTTGTGCCTC	25	
NpF1160-TH-BamHI-F	atataggatcccATGTCTTTCAAAATAGATCGTGG	26	
NpF1160-TH-KpnI-R	atataggtacccgTTTTTTCTTCCCACCAAACAAAC	27	
Npun_R3872-TH-BamHI-F	atataggatcccATGTCACAGACCTTACTACC	28	
Npun_R3872-TH-KpnI-R	atataggtacccgACACTTGACTTGAGATCCTTTTC	29	
Npun_R5997-TH-BamHI-F	atataggatcccATGCAAAATTTGCCGAATTTCC	30	
Npun_R5997-TH-KpnI-R	atataggtacccgACTCAGTAAATCAGCACGG	31	
Npun_R5579-TH-BamHI-F	atataggatcccGTGCGAATTCCGCTAGATTAC	32	
Npun_R5579-TH-KpnI-R	atataggtacccgTCTGGTGAATTGATTTACAACAG	33	
Npun_R1936-TH-BamHI-F	atataggatcccATGGCTCGCAAAAAATCACTTC	34	
Npun_R1936-TH-KpnI-R	atataggtacccgTCTCATTAATTCTAACAACATCTG	35	
Npun_R6085-TH-BamHI-F	atataggatcccATGGCTGCAACCGACTTCAAAG	36	
Npun_R6085-TH-KpnI-R	atataggtacccgCAGCTTGACTTGCTGCAAATG	37	
Npun_F0150-TH-BamHI-F	atataggatcccATGCTTACCGAATTTGACAC	38	
Npun_F0150-TH-KpnI-R	atataggtacccgACTTGTTTTCGGTTTGATGTATG	39	
NpF0123-TH-BamHI-F	atataggatcccATGGCCCGCGACTATTATG	40	

(Table 2 Continued)

NpF0123-TH-KpnI-R	atataggtacccgCTTAAATAAATTTCCCAAAAATCCTTC	41	
NpF0151-TH-BamHI-F	atataggatcccATGAGCGATCGCTTTGATATAAATC	42	
NpF0151-TH-KpnI-R	atataggtacccgGATATCGCATTGCCAAAGC	43	
Npun_F2991-TH-BamHI-F	atataggatcccATGGTTGCAGCAACCGATTTC	44	
Npun_F2991-TH-KpnI-R	atataggtacccgTAACCGCACCTCTTCTAAG	45	
Npun_F5908-TH-BamHI-F	atataggatcccATGCCAACTGCAAATGATTTC	46	
Npun_F5908-TH-KpnI-R	atataggtacccgTAACGTCACTCCTTCTAATG	47	
sll0058-TH-BamHI-F	atataggatcccATGGGCAAAGTCATTGGCATTG	48	
sll0058-TH-KpnI-R	atataggtacccgATCGATCGCTTCATAGTCAC	49	
slr0063-TH-BamHI-F	atataggatcccATGACATCTTCCTCCTCTTC	50	
slr0063-TH-KpnI-R	atataggtacccgGCTAAACCGGGAAGTCATG	51	
sll1384-TH-BamHI-F	atataggatcccATGAGCTCGTTTCCCATCAAG	52	
sll1384-TH-KpnI-R	atataggtacccgTTTCTTTTTGCCCCCGAATAAC	53	
qNpun_F0070-F2	GGTAGCCAAATTCACCCTGA	54	hpsE
qNpun_F0070-R2	TTGCCTTGAACTCTCCCAGT	55	hpsE
qNpR638-F	AGCCCATTTGGTGCATTTAG	56	hpsN
qNpR638-R	CACTTTTATGGCAGGGTGGT	57	hpsN
qNpF1388-F	GGACACCACCAAGCGTACTT	58	hpsQ
qNpF1388-R	TGTTAGTTGGTTGCGACAGG	59	hpsQ
qNpR1506-F	TAACGGTGAGGCGGATTTAC	60	hpsR
qNpR1506-R	GCGAATTGTAATTGGGCAGT	61	hpsR
qNpR5614-F	ATGCCAGACACCCAAATCTC	62	hpsS
qNpR5614-R	TTGTGGGCCCTTTGTTCTAC	63	hpsS
qNpun_r018_F2	CACAGAAAGATACCGCCAGA	64	rnpB
qNpun_r018_R2	ATACTGCTGGTGCGCTCTTA	65	rnpB
Tn5-seq-F	CGATGAAGAGCAGAAGTTATC	66	
Tn5-seq-R	GGCTCTATTCAGGATAAATC	67	
Tn5-seq-F-nest	CGTTACCATGTTAGGAGGTC	68	

RESULTS

Identifying the Cognate Partner for DnaK1

The genome of *N. punctiforme* encodes 5 proteins annotated as DnaK homologs, 14 DnaJ homologs, and a single GrpE homolog. Based on the nomenclature applied to putative DnaK and DnaJ proteins in the closely related cyanobacterium *Nostoc flagelliform* (Xu et al., 2020), we have designated the *N. punctiforme* orthologs DnaK1-4 and DnaJ1-11, and the additional non-orthologous proteins DnaK5-6 and DnaJ12-14 (Fig. 3C) As part of an on-going transposon mutagenesis screen, a non-motile isolate was identified that harbored a transposon insert in sequence for *dnaK1*. The *dnaK1* gene is encoded at a locus in between *grpE* and *dnaJ11*, with all three genes in the same orientation (Fig. 3C), implying they may comprise an operon and their protein products might form a functional chaperone system. However, previously published RNAseq data (Gonzales et al., 2019) indicates that while the expression of *grpE* and *dnaJ11* is static in developing hormogonia, expression of *dnaK1* is significantly upregulated, with a maximum increase in expression of ~32 fold at 12 h post hormogonium induction (Fig. 3B).

Figure 3

Gene Expression of DnaK-type System in Cyanobacteria

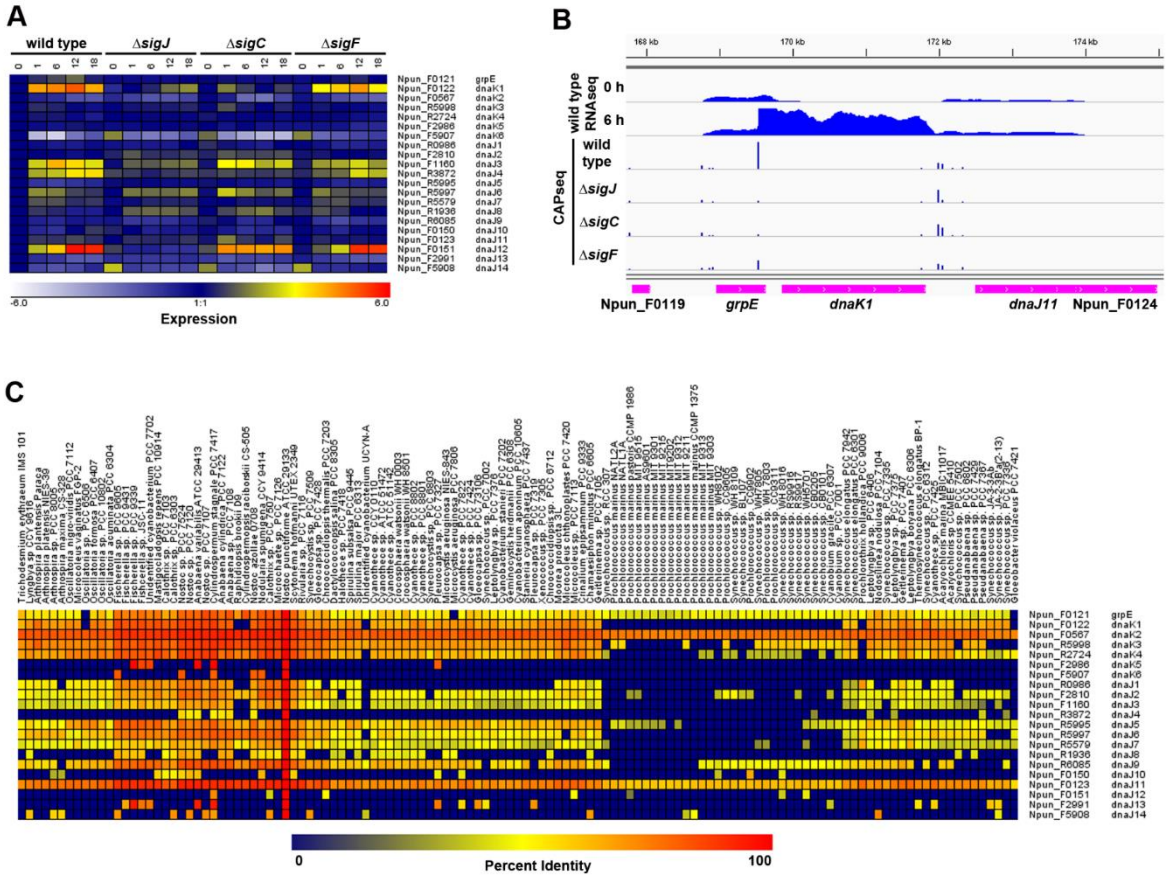

Note. Gene expression and genomic conservation of DnaK-type chaperone system components in *N. punctiforme*. **(A)** Heat maps depicting the expression of *dnaK*, *dnaJ*, and *grpE* genes in developing hormogonia of the wild-type and hormogonium-specific sigma factor mutants 0-18 h post hormogonium induction. Expression = Log2(experimental strain and time point/wild type t=0). **(B)** Read map coverage from RNAseq and Cappable-Seq data for various strains and time points as indicated. **(C)** Heat map depicting genomic conservation of genes encoding DnaK, DnaJ, and GrpE proteins among cyanobacteria.

In an effort to identify cognate DnaJ proteins for DnaK1, the transcriptional profiles of all annotated *dnaK* and *dnaJ* genes during hormogonium development were analyzed , and the phylogenetic co-occurrence of the *N. punctiforme* proteins in other cyanobacteria was investigated (Fig. 3C). Of the six *dnaK* genes, only *dnaK1* is upregulated in developing hormogonia, while the other five are either static or downregulated. Of the 14 *dnaJ* genes, three exhibited enhanced expression in developing hormogonia, *dnaJ3*, *dnaJ4*, and *dnaJ12*. For *dnaJ3* and *dnaJ12*, transcription was dependent on the presence of *sigJ*, while transcription of *dnaJ4* was dependent on both *sigJ* and *sigC*, indicating it is most directly regulated by *sigC*. The -10 region of the promoters for both *dnaJ3* and *dnaJ12* have also been shown to contain consensus J-Boxes (Harwood & Risser 2021). Based on this transcriptional data, one or more of these three DnaJ proteins may interact with DnaK1 in hormogonia.

Co-occurrence analysis of *N. punctiforme* DnaK and DnaJ proteins in other cyanobacteria indicate that both GrpE and DnaJ11, along with DnaK2, are nearly ubiquitous among the cyanobacteria investigated implying that these proteins comprise a system conserved in essentially all cyanobacteria (Fig. 3C) (Cho et al., 2017). In contrast, DnaK1 shows a distinct conservation pattern, with orthologs absent in the marine picocyanobacteria as well a few other phylogenetically dispersed species. Notably, the conservation pattern of DnaJ3 closely resembles that of DnaK1, while the other two DnaJ proteins upregulated in hormogonia are only present in a handful of other cyanobacteria (Fig. 3C). The combination of transcriptional profiles and co-occurrence for *dnaK1* and *dnaJ3* provide compelling circumstantial evidence that these proteins may be cognate partners of a chaperone system.

To provide further evidence for the correct co-chaperone to DnaK1, a bacterial adenylate cyclase two-hybrid (BACTH) assay was used to test for protein-protein interactions between

DnaK1 and all identified DnaJ proteins as well as GrpE **(**Fig. 4A). A total of thirteen DnaJ proteins were successfully co-expressed with DnaK1, with the exception of DnaJ5 as the PCR amplification of *dnaJ5* repetitively failed for unknown reasons. A positive protein-protein interaction was only detected for DnaJ2 and DnaJ3. Interestingly, DnaJ11 did not show a positive result with DnaK1 and was not further investigated. Additionally, GrpE and DnaK1 also exhibited a positive protein-protein interaction as was predicted based on previous research. These results together further support that hypothesis that DnaK1 and DnaJ3 along with GrpE work together in a chaperone system as some function in the development of hormogonia.

Figure 4
Bacterial-Two Hybrid Protein Interactions

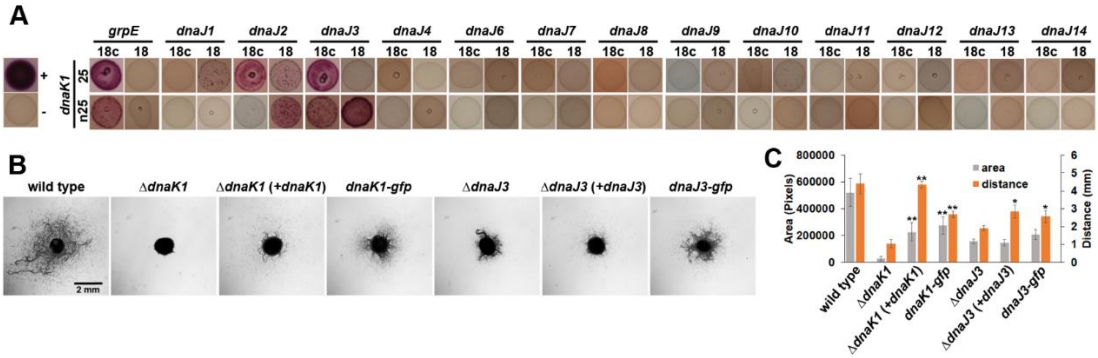

Note. Identification of the DnaK1/J3 chaperone system. **(A)** BACTH analysis between DnaK1, and GrpE or DnaJs encoded in the *N. punctiforme* genome fused to the C (25) and N (n25) terminus of the T25 fragment or C (18c) and N (18) terminus of the T18 fragment of *B. pertussis* adenylate cyclase. Depicted are the results from assays on MacConkey agar. The positive control strain (+) harbors plasmids pKT25-zip and pUT18c-zip, while the negative control strain (-) harbors the empty vectors pKT25 and pUT18c. **(B)** Plate motility assays of the wild-type, deletion strains, complemented deletion strains, and strains harboring *gfp*-tagged alleles (as

indicated). Images were taken at 48 h post hormogonium induction. **(C)** Quantification of plate motility assays depicted in B based on the area covered by a spreading colony and the maximal distance traveled by individual filaments. Error bars = +/- 1 S.D. * = p-value<0.05, **= p-value<0.01 as determined by two-tailed Student's t-Test between the *dnaK1*- or *dnaJ3*-deletion strains and the corresponding complemented or *gfp*-tagged allele strain, n=3. All strains showed reduced motility compared to the wild-type as determined by two-tailed Student's t-Test, p-value<0.05, with the exception of maximal distance for Δ*dnaK1* (+*dnaK1*).

dnaK1 and *dnaJ3* Influence Hormogonium Motility

To confirm the initial results of the transposon mutagenesis screen and further support the possible role of *dnaK1* in hormogonium development and motility, In-frame deletion of both and *dnaK1* and *dnaJ3* significantly reduced hormogonium motility in both colony spreading and time-lapse motility assays. Reduction of motility was most pronounced in the Δ*dnaK1* strain. For each deletion strain the reintroduction of the corresponding gene in trans on a replicative shuttle vector under the control of the native promoter restored motility, although slightly reduced in comparison to WT. This data along with initial observations further implies a critical role of DnaK1 and DnaJ3 in establishing functional motility as part of a normal system required during hormogonia development (Fig. 4B+C).

Figure 5

Light Microscopy and Immunoblot Analysis of ΔdnaK1 and ΔdnaJ3 Strains

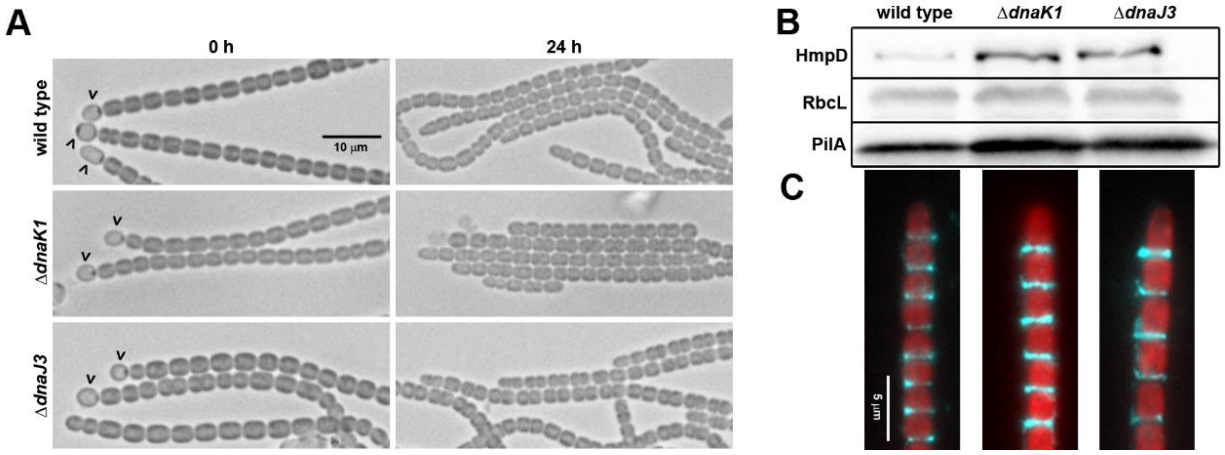

Note. Characterization of hormogonium development in the Δ*dnaK1* and Δ*dnaJ3* strains. **(A)** Light micrographs of the filament morphology for the wild type and deletion strains at 0 h and 24 h post hormogonium induction. Carets indicate the presence of heterocysts attached to filaments. Hormogonia can be distinguished from vegetative filaments by the absence of heterocysts, smaller cell size, and presence of tapered cells at the filament termini. **(B)** Immunoblot analysis of cellular HmpD, PilA, and RbcL, and **(C)** immunofluorescence analysis of extracellular PilA in the wild type and deletion strains 24 h after hormogonium induction. RbcL is the large subunit of RUBISCO and serves as a protein loading control. Depicted are merged images of fluorescence micrographs acquired using a 63x objective lens from cellular autofluorescence (red) and PilA immunofluorescence (cyan).

dnaK1 and *dnaJ3* Influence HPS Production

To further define the role of *dnaK1* and *dnaJ3*, several aspects of hormogonium development were investigated in the deletion strains (Fig 5A-C). Microscopic examination of filament morphology indicated that both deletion strains produced morphologically distinct

hormogonia (Fig. 5A). Immunoblot and immunofluorescence analysis of the hormogonium-specific proteins PilA and HmpD indicated normal expression of these proteins (Fig. 5B) and normal accumulation of PilA on the cell surface (Fig. 5C). However, lectin staining and lectin blotting indicated that both strains produce significantly less HPS than the wild-type strain (Fig. 5A), implying that *dnaK1* and *dnaJ3* play a critical role in regulating HPS production. Moreover, exogenous addition of HPS significantly enhanced the motility of both the Δ*dnaK1* and Δ*dnaJ3* strains (Fig. 6B+C), further supporting the hypothesis that deletion of *dnaK1* and *dnaJ3* leads to a specific defect in HPS production.

Figure 6

Complementation and Motility Assay of Δdnak1 and ΔdnaJ3

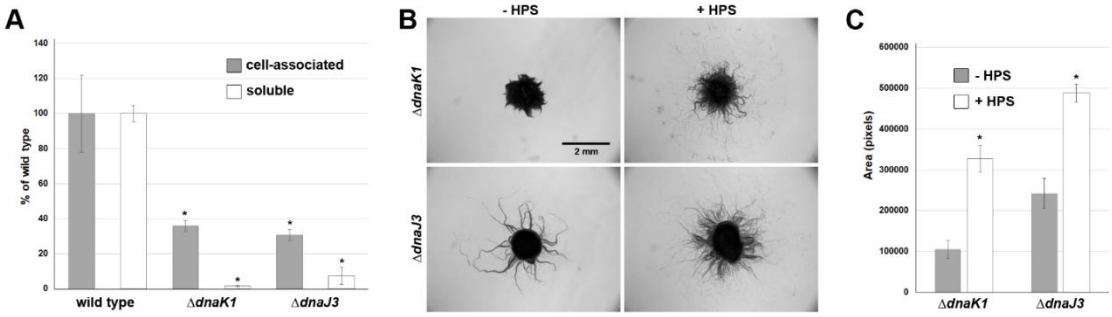

Note. *dnaK1* and *dnaJ3* are required for production of hormogonium polysaccharide **(A)** Quantification of cell-associated and soluble HPS based on fluorescent lectin staining and lectin blotting respectively. Error bars = +/- 1 S.D. * = p-value<0.05 as determined by two-tailed Student's t-Test between the wild type and each deletion strain, n=3. **(B)** Complementation of the *dnaK1* and *dnaJ3* deletion strains by exogenous addition of HPS. Depicted are plate motility assays of the deletion strains alone (-HPS) or supplemented with HPS from cell-free culture medium (+HPS). Images were taken at 48 h post hormogonium induction. **(C)** Quantification of plate motility assays depicted in B based on the area covered by a spreading colony. Error bars =

+/- 1 S.D. * = p-value<0.05 as determined by two-tailed Student's t-Test between each deletion Dstrain in the presence or absence of HPS, n=3.

To determine if DnaK1 and DnaJ3 affect HPS production at the transcriptional level, the expression of an *hps* gene from each known *hps* locus (Zuinga et al., 2020) was analyzed by RT-qPCR in the Δ*dnaK1* strain (Fig. 7). All of the genes tested displayed a robust increase in transcription 18 h post-hormogonium induction in both the wild-type and Δ*dnaK1* strains. Compared to the wild-type strain, only *hpsE* showed a detectable reduction in expression in the Δ*dnaK1* strain, but this reduction was very moderate, and *hpsE* expression still increased ~16 fold in the Δ*dnaK1* strain at 18 h compared to 0 h. In contrast, expression of *hpsS* was moderately enhanced in the Δ*dnaK1* strain compared to the wild-type. Collectively, these results imply that the reduced HPS production in the Δ*dnaK1* strain is unlikely to be a result of changes in gene expression, at least for those genes currently known to be involved in HPS synthesis.

Figure 7

Expression of hps Genes in the Δdnak1 Strain

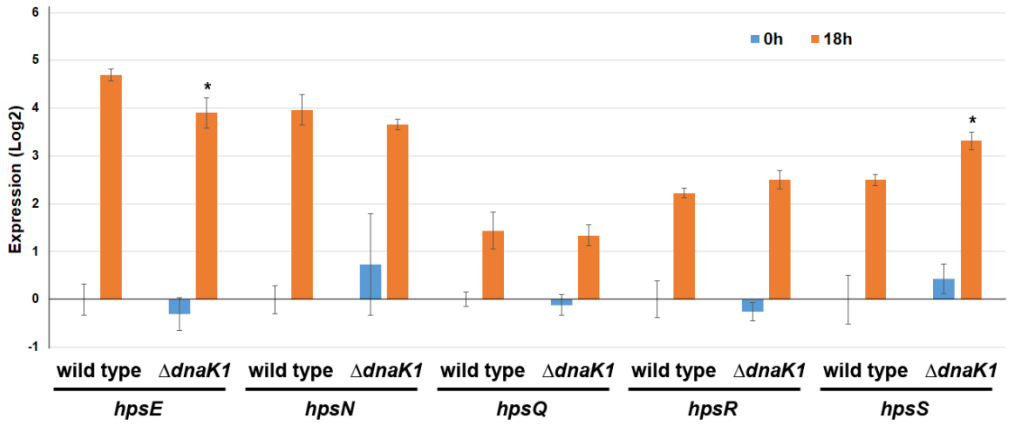

Note. Expression of *hps* genes in the Δ*dnaK1* strain. The expression of various *hps* genes from known *hps* loci was determined by RT-qPCR in the wild-type and Δ*dnaK1* strains 0 and 18 h post hormogonium induction. Error bars = +/- 1 S.D. * = p-value<0.05 as determined by two-tailed Student's t-Test between the wild type and Δ*dnaK1* strain at the corresponding time point, n=3.

DnaK1 Dynamic Interactions with T4P Motor Proteins

The DnaK1 ortholog in *N. flagelliforme* (Xu et al., 2020) was shown to interact with the cytoplasmic membrane upon induction. To further asses the cellular locations of both DnaK1 and DnaJ3 within *N. punctiforme,* strains harboring *gfp*-tagged chromosomal alleles of *dnaK1* and *dnaJ3* were analyzed by fluorescence microscopy. For both strains, GFP-derived fluorescence was not detected in undifferentiated vegetative filaments consistent with the transcriptional data indicating these genes are transcribed specifically in hormogonia (Fig. 8A). In hormogonia, DnaK1 accumulated at the leading poles of cells in motile filaments while DnaJ3 displayed bi-polar fluorescence (Fig. 8A+B). When filaments of the *dnaK1-gfp* strain were exposed to a light regimen known to trigger dynamic localization of the T4P-associated protein HmpF, which in

turn stimulates filament reversals (Harwood et al., 2021), DnaK1 exhibited dynamic localization (Fig., 8B). Upon exposure to high intensity light at 405 nm for imaging GFP, followed by subsequent incubation in the dark for 1 min, a substantial fraction of the protein dissociated from the leading pole and accumulated in the cytoplasm or at the lagging cell pole, so that cells displayed dimmer, bipolar fluorescence rather than bright unipolar fluorescence. When filaments were subsequently incubated in white light again for 1 min, the majority of the protein re-accumulated at the new leading poles of motile filaments. Immunoblot analysis with α-GFP antibodies confirmed the presence of proteins at the expected molecular weight for full-length DnaK1-GFP and DnaJ3-GFP (Fig. 9) although both strains produced lower molecular weight proteins that could be the result of degradation of the fusion proteins as well. DnaK1-GFP was also much more abundant than DnaJ3-GFP, consistent with the results from fluorescence microscopy.

The polar localization of HmpF has been shown to be disrupted by treatment with the proton-ionophore carbonyl cyanide m-chlorophenyl hydrazine (CCCP) (Harwood et al., 2021), indicating that proton motive force, or some other indirect effect of CCCP treatment modulates HmpF localization. Given the similarities in the behavior of HmpF and DnaK1, the effect of CCCP treatment on DnaK1-GFP and DnaJ3-GFP was determined. Treatment with CCCP resulted in the loss of unipolar localization and a concomitant increase in cytoplasmic localization as well as low levels of bipolar accumulation for DnaK1-GFP, but had no effect on DnaJ3-GFP localization (Fig. 8C+D). The similarities in the localization patterns for HmpF and DnaK1 could indicate that the subcellular localization of DnaK1 is influenced by the status of the T4P motors. Alternatively, the influence of light and CCCP treatment on the behavior of DnaK1 might be due to other effects on the cell such as depletion of ATP levels. To distinguish between

these possibilities, the behavior of DnaK1-GFP was determined in a strain also harboring deletion of *hmpF*, which is essential for activation of the T4P motors. In the *hmpF*-deletion strain, DnaK1-GFP localization was similar to that observed upon CCCP treatment in the wild-type genetic background, with high levels of cytoplasmic fluorescence and weak bipolar accumulation (Fig. 5C+D). Moreover, DnaK1-GFP no longer exhibited any changes in localization upon exposure to CCCP in the *hmpF* genetic background. Both quantitation of fluorescence levels and immunoblot analysis indicated that the observed changes could not be attributed to reduced expression of the DnaK1-GFP fusion protein due to deletion of *hmpF* (Fig. 8C+D, Fig. 9). These results are consistent with a model where the status of the T4P motor influences the localization of DnaK1.

To determine whether DnaK1 interacts directly with the T4P motors, the BACTH assay was employed to test for interaction between DnaK1 and various cytoplasmic-facing T4P proteins (Fig. 8E). Interactions were detected between DnaK1 and Hfq or PilB, but not HmpF, PilT1 or PilT2.

Figure 8

Localization of DnaK1 and DnaJ3 and Bacterial-Two Hybrid Results with T4P

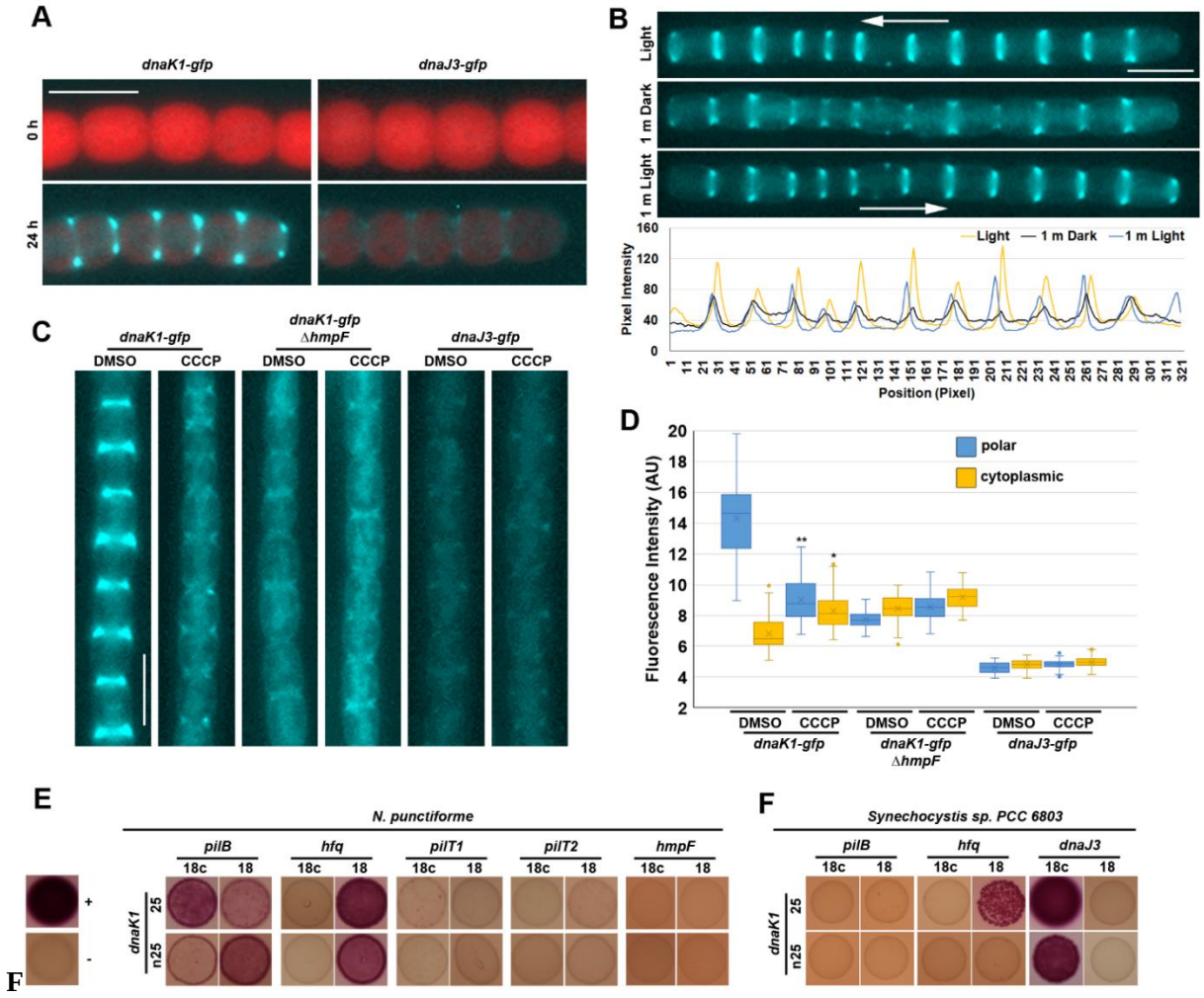

Note. Localization of DnaK1 and DnaJ3 and interaction of DnaK1 with the T4P motor complex. **(A)** Fluorescence micrographs of the *dnaK1-gfp* and *dnaJ3-gfp* strains at 0 and 24 h post hormogonium induction. Depicted are merged images of fluorescence micrographs acquired using a 63x objective lens from cellular autofluorescence (red) and GFP fluorescence (cyan) from immobilized filaments. **(B)** Dynamic localization of DnaK1-GFP in response to light in a motile filament. Depicted are fluorescence micrographs of GFP fluorescence from a motile filament of the *dnaK1-gfp* strain pre-incubated in white light for 1 min (Light), followed by

darkness for 1 min (Dark), and subsequently incubated in white light for 1 min (1 m Light). Arrow indicates the direction of movement for the filament. White bar = 5 µm. The lower panel depicts quantification of positional fluorescence intensity. Using imageJ, a line was drawn along the length of the filament and the pixel intensity was measured at the indicated time points in the light regimen. **(C)** Localization of DnaK1-GFP and DnaJ3-GFP in response to treatment with CCCP or DMSO alone in a wild-type genetic background or DnaK1-GFP in a Δ*hmpF* background. Depicted are fluorescence micrographs of GFP fluorescence (cyan). White bar = 5 µm. **(D)** Quantification of the fraction of DnaK1-GFP or DnaJ3-GFP localized to the poles and cytoplasm. * = p-value<0.05 as determined by two-tailed Student's t-Test between the CCCP and DMSO treatment for each strain and position measured, n=3. **(E)** BACTH analysis between DnaK1, and various cytoplasmic facing proteins of the T4P in *N. punctiforme* or **(F)** DnaK1 and DnaJ3 or T4P proteins from *Synechocystis* sp. strain PCC 6803. Proteins are fused to the C (25) and N (n25) terminus of the T25 fragment or C (18c) and N (18) terminus of the T18 fragment of *B. pertussis* adenylate cyclase. Depicted are the results from assays on MacConkey agar. The positive control strain (+) harbors plasmids pKT25-zip and pUT18c-zip, while the negative control strain (-) harbors the empty vectors pKT25 and pUT18c.

Figure 9

*Immunoblot analysis of WT, Δ*dnaK1, and Δ*dnaJ3*

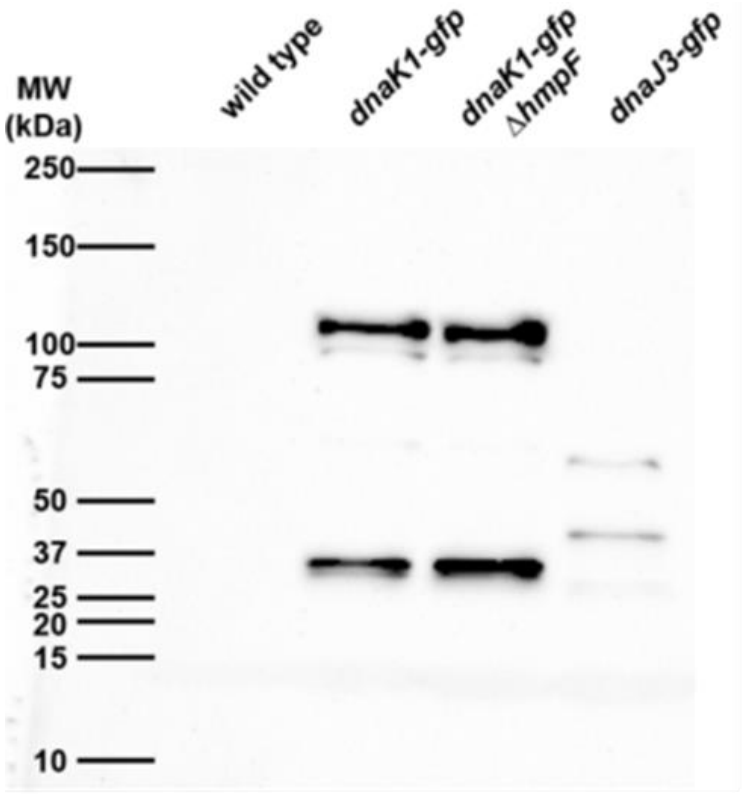

Note. Immunoblot analysis of the wild-type, Δ*dnaK1*, and Δ*dnaJ3* strains with an α-GFP antibody. Expected molecular weight of DnaK1-GFP = ~99 Kda, and DnaJ3-GFP = ~63 Kda.

DISCUSSION

Abolition of Motility and Location Within the Gene Regulatory Network

Characterization of Δ*dnaK1* and Δ*dnaJ3* further support the theory of a functional DnaK1 – DnaJ3 -GrpE HSP system upregulated in hormogonia development essential for motility within *N. punctiforme*. Light-microscopy time-lapse motility trials of Δ*dnaK1* and Δ*dnaJ3* showed intact hormogonium filaments with reduced motility. However, aggregated filaments displayed significantly more twitching and longitudinal movement. This slight conservation of motility is most likely due to the presence of small amounts of hormogonium polysaccharide within the clump of hormogonium filaments. The later exogenous addition of hormogonium polysaccharide to non-motile filaments further increased motility in both Δ*dnaK1* and Δ*dnaJ3.* Conserved movement of these aggregate filaments with similar wild-type secretion levels of PilA suggests that one of the primary factors contributing to the motility disruption within Δ*dnaK* and Δ*dnaJ3* is the lack of hormogonium polysaccharide production and secretion.

The hormogonium phenotype was also retained among both the Δ*dnaK1* and Δ*dnaJ3* mutants expanding the gene regulatory network to predict *dnaK1* as downstream of several key developmental proteins including the previously discussed hybrid histidine kinase HrmK and the trio of sigma factors SigJ, SigC and SigF. However, it is important to note that while the approximate location of *dnaK1* in the GRN may possibly be derived from these findings, the exact regulation and function of DnaK1 in hormogonia is still unknown. Given the broad capabilities of Heat-Shock Protein systems it is not unlikely that this specific system interacts with other currently unidentified proteins possibly affecting further downstream targets. This theory is further bolstered by evidence of a protein-protein interaction between DnaK1 and

DnaJ2, a JDP not shown to be upregulated during the development of hormogonium. This interaction could be explained by the characteristic lack of binding specificity of JDP as evidenced by previous research in *Nostoc flagelliform* (Xu et. al. 2020). However, it is also likely that DnaJ2 may serve several functions in the various cell types of *N. punctiforme* and possibly performing a regulatory role in the hormogonium as a part of an HSP system with DnaK2. Further research is needed to fully elucidate the role and other proteins targets of DnaK2 as a part of the HSP system.

Positive protein-protein interactions between DnaK2 and T4P motor proteins PilB and Hfq present the possibility of a role in hormogonium polysaccharide secretion influenced by protein binding at or near the poles. As was previously discussed, association of HmpF with the T4P motor proteins activates the extension and retraction of the T4P and the secretion of PilA. These same motor proteins that interact with DnaK1 appear to affect the secretion and production hormogonium polysaccharide in a similar way. It is important to note that DnaK1 did not show a positive interaction with HmpF indicating a possible separate system of influence over the activation of T4P proteins.

Localization of DnaK1 and DnaJ3

The dynamic localization of DnaK1 in response to light conditions indicates a possible relationship between this HPS system and the Hmp or Ptx systems in *N. punctiforme.* The light-dark trials of induced GFP-DnaK1 clearly show the clustering of DnaK1 at the pole of forward movement during light conditions and a delocalization into the cytoplasm when light is obscured. No evidence of fluorescence by GFP-DnaK1 was observed in vegetative filaments further supporting the conclusion that transcription and translation of *dnaK2* is initiated by the GRN for the induction of hormogonia. Inhibition of the Hmp system by CCCP abolished the

directionality and polar specificity of DnaK1 in vivo in both light and dark conditions. While cellular bi-polar T4P protein concentrations remain the same at each pole, the lack of DnaK1 binding implies a possible disruption of the known T4P/DnaK1 protein-protein interactions in response to changed in light. Furthermore, there is no evidence for a direct interaction between HmpF and DnaK1. We postulate that HmpF may indirectly influence the polar recruitment of DnaK1 in response to light but cannot rule out an alternative influence by the Hmp or Ptx systems in general.

Working Model of the DnaK/DnaJ Chaperone System

Based on the evidence provided in this research we propose a working model for how the DnaK1/J3 influences HPS production in response to T4P activity (Fig. 10). The association of HmpF with the T4P motor proteins activates pilus extension and retraction at the leading pole. DnaK1 is then subsequently recruited to the active motor where HmpF is theoretically bound and forms a protein complex with DnaJ3 that serves as a functional HSP70 system to regulate the folding of an unidentified protein. This protein then will promote the production of hormogonium polysaccharide through an unknown mechanism. Given that DnaJ2 also interacts with DnaK1, it is possible there is another protein target or functional component to this system at the cell poles. However, unlike DnaK1 and DnaJ3, DnaJ2 is not specifically expressed in hormogonia. Further experiments will be needed to determine the role of DnaJ2 in the regulation of hormogonium polysaccharide production and secretion, if any.

Figure 10

Working Model of DnaK1/DnaJ3 Chaperone System

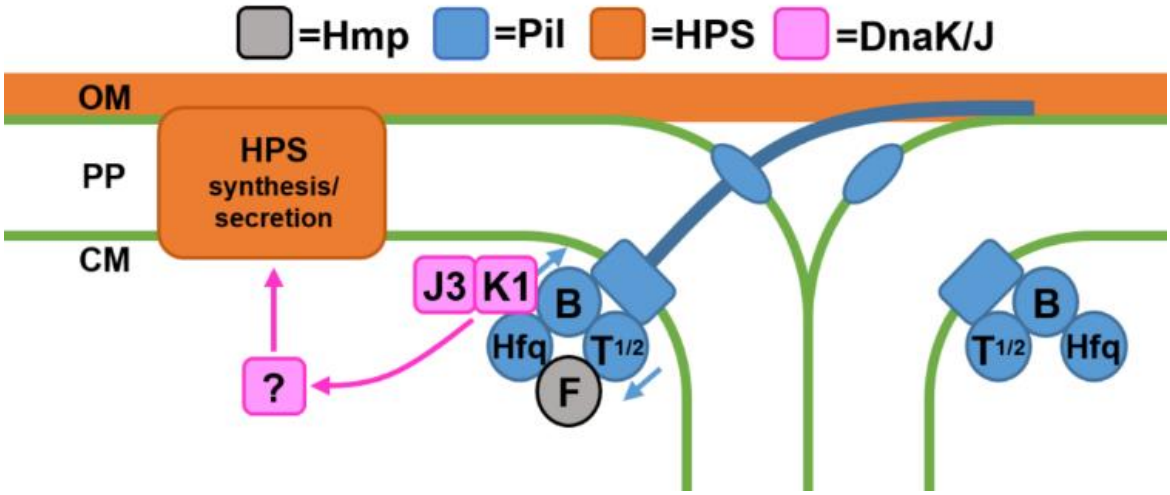

Note. A working model of how the DnaK1/DnaJ3 chaperone system coordinates T4P activity and HPS production. Association of HmpF with the T4P motors activates cycles of pilus extension and retraction at the leading poles of cells. DnaK1 is subsequently recruited to the active motors via interaction with PilB and Hfq, where it forms a functional chaperone system influencing the folding state of an unidentified protein, which in turn influences production of HPS. OM = outer membrane, PP = periplasm, CM = cytoplasmic membrane.

The complete mechanism of HPS secretion is still missing several key factors, most notably the bridge between the motor proteins of the T4P and the activation of HPS production and secretion. Furthermore, the expression of genes associated with secretion of HPS do not appear to be affected by the absence of *dnaK1* as evidenced by RT-qPCR expression levels of the HPS locus genes from the Risser lab in 2021. Most likely there is no regulation of HPS secretion by *dnaK1* at the transcriptional level. There is quite possibly another completely unknown system responsible for the expression of regulation of the genes and proteins that affect

HPS production and secretion in hormogonium that also interact with DnaK1. Further research into protein level expression and functionality is needed to elucidate the relationship between DnaK1 and the HPS secretion system.

Given the conserved nature of DnaK1 and the essential function of T4P regulation in *N. punctiforme*, this protein-protein network may influence T4P activation in a similar manor across the filamentous and unicellular cyanobacteria species. The ubiquitous nature of *dnaK1* may indicate an early evolution of this specific system within cyanobacteria. The evolution of the chemotaxis-like movement of *N. punctiforme* multicellular filaments in response to light is essential for acquisition of nutrients and plant symbioses. Without this complex response to light and pilus extension, photosynthesis and nutrient exchange with plants would not be optimized for *N. punctiforme*.

The correlation of the GOE with the appearance of filamentous cyanobacteria (Schirrmeister et al., 2013) in Earth's history stresses the importance of heat-shock protein systems to regulate motility function with an unpredictable atmosphere. As was previously discussed HSP70-like proteins are identified not only in heat stress responses but to other types of stress like desiccation and nutrient deficiency. The multicellularity and filamentous nature of cyanobacteria as regulated by natural light enables photosynthesis while avoiding excess exposure to UV. The evolution of the DnaK1 system in *N. punctiforme* may therefore have played a crucial role in the evolution of atmospheric oxidation and the development of more complex multicellular life forms.

Future Implications

Further developing the gene regulatory model of hormogonium development may have many future implications in the fields of biotechnology. The growing land and nutrient demands

in agriculture to sustain the expanding human and livestock populations increases the demand for chemical fertilizers to maximize crop production. Soil nitrogen does not rapidly replenish with modern farming technology and must be augmented through fertilization or crop rotations. A potential alternate to the mass use of synthetic fertilizers is the integration of augmented nitrogen-fixing strains of cyanobacteria into crop soil. Synthetic fertilizers are well known to toxify the surrounding ecology and frequently pollute important water sources through "run off". The potential to genetically engineer cyanobacteria that integrate into essential crop soil may reduce the ecological impact of fertilizations and potentially provide a more sustainable and longer solution to soil nitrogen depletion. Biofuel development as an alternate solution to traditional fossil or gas fuels may provide a sustainable solution to non-renewable sources of energy. Through bioengineering and ongoing research algae and cyanobacteria are considered sources of "clean energy" as they do no accumulate significant biomass or toxic byproducts. *Nostoc sp.* will continue to photosynthesis in their motile form without significant cellular growth or mass accumulation. Successful experimentation with cyanobacteria in the production of fuels has already produced some success with the successful production of ethanol and isoprene on a small scale (Luan and Lu, 2018).

More recently, the investigation into cyanobacteria and their potential importance in ecosystem monitoring and restoration ecology further emphasizes the importance of research into the function mechanisms of the key species. Seed-based restoration efforts after wildfires rely on successful indigenous plant recruitment to restore devastated ecosystems. The presence of healthy native soil microbial communities after a wildfire influences the success rates of new seedlings. Efforts to artificially repopulate native soils with symbiotic and photosynthetic bacteria like cyanobacteria may greatly increase the rate at which ecosystems recover (Dadzie et

al., 2022). Soil salinization as a consequence global warming may also be a target of ecosystem restoration efforts by Cyanobacteria. Distributed over broad range of salt concentration and fluctuation salinity levels that, certain species of Cyanobacteria and specifically *Nostoc sp*. have demonstrated a mechanism of osmotic acclimation through the production of an extracellular polysaccharide that binds sodium ions and produces a protective biofilm. This biofilm serves to protect not only the bacterial colony but also the surrounding plants from fluctuating salt levels. In addition to the biofilm, *Nostoc sp*. may also produce trichomes that remove soluble sodium from their aqueous environment though bio-absorption (Rocha et al., 2020).The potential applications of cyanobacteria in combating climate change and ecosystem destruction are ever expanding.

References

1. Adams DG, Carr NG.The developmental biology of heterocyst and akinete formation in cyanobacteria. **(1981)** Crit Rev Microbiol. 9(1):45-100
2. Battesti A & Bouveret E The bacterial two-hybrid system based on adenylate cyclase reconstitution in escherichia coli. **(2012)** *Methods* 58(4): 325-334.
3. Bhaya D, Takahashi A, Shahi P & Grossman AR Novel motility mutants of synechocystis strain PCC 6803 generated by in vitro transposon mutagenesis. **(2001)** *J Bacteriol* 183(20): 6140-6143.
4. Black WP, Xu Q & Yang Z Type IV pili function upstream of the dif chemotaxis pathway in myxococcus xanthus EPS regulation. **(2006)** *Mol Microbiol* 61(2): 447-456.
5. Borrero-de Acuña José Manuel, *et al* A periplasmic complex of the nitrite reductase NirS, the chaperone DnaK, and the flagellum protein FliC is essential for flagellum assembly and motility in pseudomonas aeruginosa. **(2015)** *J Bacteriol* 197(19): 3066-3075.
6. Cai YP & Wolk CP Use of a conditionally lethal gene in anabaena sp. strain PCC 7120 to select for double recombinants and to entrap insertion sequences**. (1990)** *J Bacteriol* 172(6): 3138-3145.
7. Campbell EL, Summers ML, Christman H, Martin ME & Meeks JC Global gene expression patterns of nostoc punctiforme in steady-state dinitrogen-grown heterocyst-containing cultures and at single time points during the differentiation of akinetes and hormogonia. **(2007)** *J Bacteriol* 189(14): 5247-5256.
8. Castenholz RW in *The Biology of Cyanobacteria,* (**1982)** eds Carr NG & Whitton BA Blackwell scientific publications, pp 413-419.
9. Cho YW, *et al* Dynamic localization of HmpF regulates type IV pilus activity and directional motility in the filamentous cyanobacterium nostoc punctiforme. **(2017)** *Mol Microbiol* 106(2): 252-265.
10. Dadzie et al Native bacteria can influence seedling emergency and groth of native plants used in dryland restoration. **(2022)** J Appl Ecol. 2022;59:2983–2992.
11. Edelstein AD, *et al* Advanced methods of microscope control using muManager software. **(2014)** *J Biol Methods* 1(2): e10.
12. Gonzalez A, Riley KW, Harwood TV, Zuniga EG & Risser DD A tripartite, hierarchical sigma factor cascade promotes hormogonium development in the filamentous cyanobacterium nostoc punctiforme. **(2019)** *mSphere* 4(3): 10.1128/mSphere.00231-19.
13. Harwood TV & Risser DD The primary transcriptome of hormogonia from a filamentous cyanobacterium defined by cappable-seq. **(2021)** *Microbiology (Society for General Microbiology)* 167(11)
14. Harwood TV, Zuniga EG, Kweon H & Risser DD The cyanobacterial taxis protein HmpF regulates type IV pilus activity in response to light. **(2021)** *Proc Natl Acad Sci U S A* 118(12): 10.1073/pnas.2023988118.
15. Harwood TV, Zuniga EG, Kweon H, Risser DD The cyanobacterial taxis protein HmpF regulates type IV pilus activity in response to light **(2021)** PNAS 2021 Vol. 118 No. 12 e2023988118
16. Holland HD. Volcanic gases, black smokers, and the great oxidation event. (**2002)** Geochimica Et Cosmochimica Acta. 66(21):3811-26.

17. Imamoglu, Rahmi, Balchin, David, Hayer-Hartl, Manajit & Hartl, F. Bacterial Hsp70 resolves misfolded states and accelerates productive folding of a multi-domain protein**. (2020)** Nature Communications. 11. 365. 10.1038/s41467-019-14245-4.
18. Jakob A, *et al* The (PATAN)-CheY-like response regulator PixE interacts with the motor ATPase PilB1 to control negative phototaxis in the cyanobacterium synechocystis sp. PCC 6803. **(2020)** *Plant Cell Physiol* 61(2): 296-307.
19. Karimova G, Pidoux J, Ullmann A & Ladant D A bacterial two-hybrid system based on a reconstituted signal transduction pathway. **(1998)** *Proc Natl Acad Sci U S A* 95(10): 5752-5756.
20. Khayatan B, *et al* A putative O-linked beta-N-acetylglucosamine transferase is essential for hormogonium development and motility in the filamentous cyanobacterium nostoc punctiforme. **(2017)** *J Bacteriol* 199(9): 10.1128/JB.00075-17. Print 2017 May 1.
21. Khayatan B, Meeks JC & Risser DD Evidence that a modified type IV pilus-like system powers gliding motility and polysaccharide secretion in filamentous cyanobacteria. **(2015)** *Mol Microbiol* 98(6): 1021-1036.
22. Livak KJ & Schmittgen TD Analysis of relative gene expression data using real-time quantitative PCR and the $2^{-\Delta\Delta CT}$ method. **(2001)** *Methods* 25(4): 402-408.
23. Luan G, Lu X. Tailoring cyanobacterial cell factory for improved industrial properties. Biotechnology Advances. **(2018)**
24. Maier B & Wong GCL How bacteria use type IV pili machinery on surfaces. **(2015)** *Trends Microbiol* 23(12): 775-788.
25. Mayer MP & Gierasch LM Recent advances in the structural and mechanistic aspects of Hsp70 molecular chaperones. **(2019)** *J Biol Chem* 294(6): 2085-2097.
26. McFadden GI. Origin and evolution of plastids and photosynthesis in eukaryotes. **(2014)** Cold Spring Harb Perspect Biol. 6(4):a016105.
27. Meeks JC, Campbell EL, Summers ML & Wong FC Cellular differentiation in the cyanobacterium nostoc punctiforme. **(2002)** *Arch Microbiol* 178(6): 395-403.
28. Meeks JC, Elhai J. Regulation of cellular differentiation in filamentous cyanobacteria in free-living and plant-associated symbiotic growth states. **(2002)** Microbiol Mol Biol Rev. 66(1):94 -121.
29. Morioka AK, Yamanaka K, Mizunoe, Y, Ogura T, Sugimoto S, Novel strategy for biofilm inhibition by using small molecules targeting molecular chaperone DnaK **(2014)** *Antimicrobial Agents and Chemotherapy* 59:633-641 doi:10.1128/AAC.04465-14

30. Nisbet EG, Grassineau NV, Howe CJ, Abell PI, Regelous M, Nisbet RERThe age of rubisco: The evolution of oxygenic photosynthesis. **(2007).** Geobiology. 5(4):311-35
31. Okuda J, *et al* The pseudomonas aeruginosa dnaK gene is involved in bacterial translocation across the intestinal epithelial cell barrier. **(2017)** *Microbiology (Society for General Microbiology)* 163(8): 1208-1216.
32. Perez-Burgos M, *et al* Characterization of the exopolysaccharide biosynthesis pathway in myxococcus xanthus. **(2020)** *J Bacteriol* 202(19): 10.1128/JB.00335-20. Print 2020 Sep 8.
33. Pratte BS & Thiel T Comparative genomic insights into culturable symbiotic cyanobacteria from the water fern azolla. **(2021)** *Microb Genom* 7(6): 10.1099/mgen.0.000595.

34. Rastogi RP, Madamwar D, Incharoensakdi A. Bloom Dynamics of Cyanobacteria and Their Toxins: Environmental Health Impacts and Mitigation Strategies. **(2015)** *Front Microbiol*. 2015;6:1254.. doi:10.3389/fmicb.2015.01254
35. Riley KW, Gonzalez A & Risser DD A partner-switching regulatory system controls hormogonium development in the filamentous cyanobacterium nostoc punctiforme. **(2018)** *Mol Microbiol* 109(4): 555-569.
36. Rippka R, Castenholz RW & Herdman M in *Bergey's manual of systematic bacteriology*, eds Boone DR, Castenholz RW & Garrity GM **(2001)** (Springer, pp 562-589.
37. Risser DD & Meeks JC Comparative transcriptomics with a motility-deficient mutant leads to identification of a novel polysaccharide secretion system in nostoc punctiforme. **(2013)** *Mol Microbiol* 87(4): 884-893.
38. Risser DD & Meeks JC Comparative transcriptomics with a motility-deficient mutant leads to identification of a novel polysaccharide secretion system in nostoc punctiforme. **(2013)** *Molecular Microbiology* 87(4): 884-893.
39. Risser DD, Chew WG & Meeks JC Genetic characterization of the hmp locus, a chemotaxis-like gene cluster that regulates hormogonium development and motility in nostoc punctiforme. **(2014)** *Mol Microbiol* 92(2): 222-233.
40. Risser DD, Wong FC & Meeks JC Biased inheritance of the protein PatN frees vegetative cells to initiate patterned heterocyst differentiation. **(2012)** *Proc Natl Acad Sci U S A* 109(38): 15342-15347.
41. Rocha, Francisco, Manuel Esteban Lucas-Borja, Paulo Pereira, and Miriam Muñoz-Rojas. "Cyanobacteria as a Nature-Based Biotechnological Tool for Restoring Salt-Affected Soils" (**2020)** Agronomy 10, no. 9: 1321. https://doi.org/10.3390/agronomy10091321
42. Rupprecht E, Gathmann S, Fuhrmann E & Schneider D Three different DnaK proteins are functionally expressed in the cyanobacterium synechocystis sp. PCC 6803. **(2007)** *Microbiology (Society for General Microbiology)* 153(6): 1828-1841.
43. Schirrmeister BE, Gugger M, Donoghue PC. Cyanobacteria and the great oxidation event: Evidence from genes and fossils. **(2015)** Palaeontology. 58(5):769-85.
44. Schuergers N, *et al* Binding of the RNA chaperone hfq to the type IV pilus base is crucial for its function in synechocystis sp. PCC 6803. **(2014)** *Mol Microbiol* 92(4): 840-852.
45. Schuergers N, Mullineaux CW & Wilde A Cyanobacteria in motion. **(2017)** *Curr Opin Plant Biol* 37: 109-115.
46. Shepard RN & Sumner DY Undirected motility of filamentous cyanobacteria produces reticulate mats. **(2010)** *Geobiology* 8(3): 179-190.
47. Splitt S & Risser D The non-metabolizable sucrose analog sucralose is a potent inhibitor of hormogonium differentiation in the filamentous cyanobacterium nostoc punctiforme. **(2015)** *Arch Microbiol* : 1-11.
48. Sugimoto S, *et al* Hierarchical model for the role of J-domain proteins in distinct cellular functions. **(2021)** *J Mol Biol* 433(3): 166750.
49. Thurotte A, Seidel T, Jilly R, Kahmann U, Schneider D. DnaK3 Is Involved in Biogenesis and/or Maintenance of Thylakoid Membrane Protein Complexes in the Cyanobacterium *Synechocystis* sp. PCC 6803. **(2020)** *Life (Basel)*. 2020;10(5):55.. doi:10.3390/life10050055

50. Tzubari Y, Magnezi L, Be'er A & Berman-Frank I Iron and phosphorus deprivation induce sociality in the marine bloom-forming cyanobacterium trichodesmium. **(2018)** *Isme J*
51. Ursell T, Chau RM, Wisen S, Bhaya D & Huang KC Motility enhancement through surface modification is sufficient for cyanobacterial community organization during phototaxis. **(2013)** *PLoS Comput Biol* 9(9): e1003205.
52. Wei TF, Ramasubramanian TS & Golden JW Anabaena sp. strain PCC 7120 ntcA gene required for growth on nitrate and heterocyst development. **(1994)** *J Bacteriol* 176(15): 4473-4482.
53. Wiltbank LB & Kehoe DM Diverse light responses of cyanobacteria mediated by phytochrome superfamily photoreceptors. **(2019)** *Nat Rev Microbiol* 17(1): 37-50.
54. Wolk CP, Cai Y & Panoff JM Use of a transposon with luciferase as a reporter to identify environmentally responsive genes in a cyanobacterium. **(1991)** *Proceedings of the National Academy of Sciences* 88(12): 5355-5359.
55. Wuichet K & Zhulin IB Molecular evolution of sensory domains in cyanobacterial chemoreceptors. **(2003)** *Trends Microbiol* 11(5): 200-203.
56. Xu HF, *et al* Dehydration-induced DnaK2 chaperone is involved in PSII repair of a desiccation-tolerant cyanobacterium. **(2020)** *Plant Physiol* 182(4): 1991-2005.
57. Yegorov Y, *et al* A cyanobacterial component required for pilus biogenesis affects the exoproteome. **(2021)** *mBio* 12(2): 10.1128/mBio.03674-20.
58. Zhang X & Bremer H Control of the escherichia coli rrnB P1 promoter strength by ppGpp. **(1995)** *J Biol Chem* 270(19): 11181-11189.
59. Zhaomin Y, Yongzhi G & Wenyuan S A DnaK homolog in myxococcus xanthus is involved in social motility and fruiting body formation. **(1998)** *J Bacteriol* 180(2): 218-224.
60. Zuniga EG, *et al* Identification of a hormogonium polysaccharide-specific gene set conserved in filamentous cyanobacteria. **(2020)** *Mol Microbiol* 114(4): 597-608.